Asian Journal of Information Technology 4 (12): 1170-1176, 2005

Design of Model Blasting for Evaluating Bench Slope Stability

Rabah Chain and Korichi Talhi
Département des Mines Faculté des Sciences de la Terre -Université de Badji Mokhtar Annaba Algérie

Abstract: This study analysed the behaviour of the rock after the blast. It is divided into two parts. The first past describes the rock behaviour law, where the ground is supposed to be in an elastoplastic model,in which are formed in the up grade bench three zones: zone of large discontinuities (the plastic zone near the drilling), the zone of small discontinuities (second plastic zone) and beyond it an elastic zone develops. The bench slope stability requires the reduction of the first plastic zone. The radius of that zone is determined as a function to the static strain energy as well as the dynamic energy resulting respectively from the static pressure p in the drilling hole and from the introduced explosive quantity. In the second part the radius is calculated as a function to the explosive quantity charge into the hole and equally on site.

Key words: Equivalent energy, strain, pressure, explosive charge, plastic zone, blasthole, slope

INTRODUCTION

Stable slopes have an important effect on surface mines working profitability, where it is necessary to take into account the safety, the environment and maintenance during exploitation. It is however known that only one part of the energy released by the explosive is used in the fragmentation process. The rest leading various harmful affect on and outside the site. In spite of the diversity of factors influencing the surface mines slope stability and various physicomechanical properties of the rock, the mining companies continue to use the same methods of the blast parameters calculation. They did not take into account the energy released by the explosive charge, and use of loading explosive into the hole and continue using identical charges with highly energies explosive (marmanite) and less energetic explosives ANFO.

This study relates to the optimisation of the blast parameters in order to obtain best fragmentation and control the rock mass behaviour, particularly the explosive powder factor.

PLASTIC ZONE RADIUS CALCULATION AS A FUNCTION TO THE EQUIVALENT STATIC ENERGY

Calculation of the strain energy: The calculation result of the stress was obtained from a drilling radius in a rock (r_t) to which a pressure was applied by a blast causing the destructuration of the rock. Since the shocks are weak (0.5 GPa < p<20 GPa), according to[1,2] the rock will behave in an elastoplastic state.

According to[3-5], three zones around the borehole are formed (Fig. 1)

- The zone of great discontinuities (plastic zone near the drilling): In this zone the breakage occurs between the tangential stress $ó_e$ and the radial stress $ó_r$, i.e. between the radius r_t (radius of drilling) and b (external radius of the zone of great discontinuities).
- The zone of small discontinuities (second plastic zone): This zone is situated between the tangential stress $ó_e$ and the vertical stress $ó_z$, i.e. between the radius b and c (external radius of the zone of small discontinuities).
- Beyond this an elastic zone develops.

Calculation of the stresses in the elastic zone: According to[6], the condition of equilibrium in the horizontal plane is:

$$\sigma_\theta - \sigma_r - r.\frac{\partial \sigma_r}{\partial r} = 0 \qquad (1)$$

σ_θ: Tangential stress
σ_r: Radial stress

The stresses are positive in compression and negative in tension.

Radial and tangential stresses in the elastic zone as writtenin the following manner:

$$\sigma_\theta = \lambda\frac{\partial u}{\partial r} + (\lambda + 2\mu)\frac{u}{r} + \lambda\varepsilon_z$$

$$\sigma_r = (\lambda + 2\mu)\frac{\partial u}{\partial r} + \lambda\frac{u}{r} + \lambda\varepsilon_z \qquad (2)$$

$$\frac{\partial \sigma_r}{\partial r} = (\lambda + 2\mu)\frac{\partial^2 u}{\partial r^2} + \lambda\frac{\partial u}{\partial r} - \lambda\frac{u}{r^2}$$

Corresponding Author: Rabah Chain, Département des Mines Faculté des Sciences de la Terre -Université de Badji Mokhtar Annaba Algérie, Tel: 00213 38 87 15 91

The coefficient of Lamé which are defined by:

$$\lambda=\frac{E\nu}{(1+\nu)(1-2\nu)}$$

$$\mu=\frac{E}{2(1+\nu)}$$

E : Young modulus
v : Poisson's ratio
λ,μ : coefficients of Lamé
The Eq. 1 becomes

$$r^2\frac{\partial^2 u}{\partial r^2}+r\frac{\partial u}{\partial r}-u=0 \quad (3)$$

The solution of the differential Eq. 3 integrated with the $c_1$constant is:

$$u=\frac{c_1}{r}+c_2 r \quad (4)$$

For an infinite radius 'r' the displacement u = 0 and c_2=0 consequently the Eq 4 becomes

$$u=\frac{c_1}{r} \quad (5)$$

For the radius limits 'c' between the elastic and plastic zones, the ultimate equilibrium is reached when the Mohr Coulomb criterion is null:

$$F(\sigma)=\sigma_r-\sigma_\theta-\sin\varphi(\sigma_r+\sigma_\theta)-2\ C.\cos\varphi \quad (6)$$

Where φ and C are, respectively the friction angle and the cohesion of the rock.

We substitute the relation (5) into the Eq 2. We point out tat for an infinite radius, the radial stress is related to the vertical stresses by the coefficient of the ground in equilibrium k_0:

$$\sigma_r=-2\mu\frac{c_1}{r^2}+k_0\sigma_z$$
$$\sigma_\theta=2\mu\frac{c_1}{r^2}+k_0\sigma_z \quad (7)$$

$$\sigma_r-\sigma_\theta=4\mu\frac{c_1}{r^2}$$
$$\sigma_r+\sigma_\theta=2K_0\sigma_2 \quad (8)$$

We substitute the relation 8 into the Eq 6, we deduct for r =c

$$CI=-\frac{c^2}{2\mu}(k_0\sigma_z\sin\varphi+C.\cos\varphi) \quad (9)$$

Elastic displacement ' u' given by the Eq. 5 which becomes

$$u=-\frac{c^2}{2\mu.r}(k_0\sigma_z\sin\varphi+C.\cos\varphi) \quad (10)$$

With the radius r = c and from relations (7) we deduct

$$\sigma_{rc}=(k_0\sigma_z\sin\varphi+C\cos\varphi+k_0\sigma_z)$$
$$\sigma_{\theta c}=-(k_0\sigma_z\sin\varphi+C\cos\varphi-k_0\sigma_z) \quad (11)$$

Before the destructuration, at the plastic radius limits r = c, we still have an elastic equilibrium

$$u_c=-\frac{c}{2\mu.}(k_0\sigma_z\sin\varphi+C.\cos\varphi)$$

For r = c the tangential and radial strains are defined

$$\varepsilon_{\theta c}=-\frac{u_c}{c},\ \varepsilon_{zc}=\frac{c_1}{c^2}\ \text{avec}\ u=\frac{c^2}{r} \quad (12)$$

We substitute the Eq. 10 and 9 into the Eq. 12 we obtain:

$$\varepsilon_{\theta c}=-\frac{1}{2\mu}(k_0\sigma_z\sin\varphi+C.\cos\varphi)$$

$$\varepsilon_{\theta c}=\frac{1}{2\mu}(k_0\sigma_z\sin\varphi+C.\cos\varphi) \quad (13)$$

After destructurationin the limit of the plastic zone, the cohesion C_f is supposed to be null and the friction angle φ_f is superior to zero.
The Eq. 13 becomes:

$$\varepsilon_{\theta cf}=-\frac{1}{2\mu_f}(k_0\sigma_z\sin\varphi f) \quad (14)$$

$$\varepsilon_{zcf}=\frac{1}{2\mu_f}(k_0\sigma_z\sin\varphi f) \quad (15)$$

But there is also a plastic equilibrium

$$\varepsilon_r^p=-n\Psi\varepsilon_\theta^p+C_3 \quad (16)$$

We substitute the Eq 14 and 15 into the Eq 16 we obtain in particular with the radius r = c,

$$C_3=\frac{1}{2\mu_f}(k_0\sigma_z\sin\varphi f)(1-n_\psi) \quad (17)$$

Plastic zone near to drilling: Between the radius of drilling r = a and the radius r = b delimiting the zone of great discontinuities, the rock is pulverulent and non-cohesive, characterized by a friction φ_f equal to inter granular friction φ_μ..

The plastic range is reached when Mohr Coulomb criterion is null, i.e.

$$F(\sigma)=\sigma_r-\sigma_\theta-\sin\varphi_\mu(\sigma_r+\sigma_\theta) \quad (18)$$

Then we deduct the ratio for the stresses:

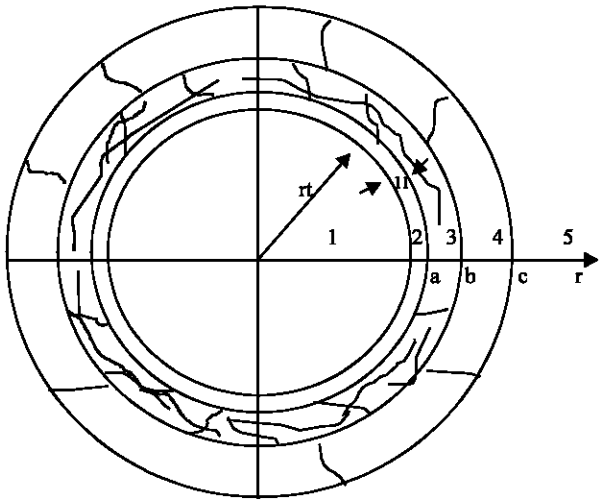

Fig. 1: Three zones around the borehole are formed

$$\frac{\sigma_\theta}{\sigma_r} = \frac{1-\sin\varphi_\mu}{1+\sin\varphi_\mu} = N_f \tag{19}$$

Consequently the Eq. 1 will have the following form:

$$N_f.\,\sigma_r - \sigma_r - r.\frac{\partial\sigma_r}{\partial r} = 0 \tag{20}$$

By integration the pressure applied to drilling ' p' at the boundaries r = a and r = b with the radial stress σ_{rb}, we will have

$$\ln\left(\frac{b}{a}\right) = \frac{1}{N_f - 1}.\ln\left(\frac{\sigma_{rb}}{p}\right) \tag{21}$$

$$b = a\left(\frac{\sigma_{rb}}{p}\right)^{\frac{1}{N_f - 1}} \tag{22}$$

Intermediate plastic zone: For r = c and according to the Mohr-Coulomb criterion (6), the rock starts to be plasticized and reaches its strength limit.
In this zone, we will admit:

- A non standard plasticity with a dilatancy Ψ determined by[7] relation related to inter granular friction φ_μ

$$\Psi = \varphi - \varphi_\mu \tag{23}$$

- A constant inter granular friction angle
- An internal friction angle and a cohesion which are degraded with the proportionally strain dilatancy

The assumption of non standard plasticity gives the following relation:

$$\vec{d}_\varepsilon^{\,p} = \xi.\frac{\partial\vec{G}(\sigma)}{\partial\sigma}$$

With G(σ), plastic potential function of the same form than F(σ):

$$G(\sigma) = \sigma_r - \sigma_\theta - \sin\Psi(\sigma_r + \sigma_\theta) \tag{24}$$

This last assumption implies that the plastic strains are of following form:

$$\begin{Bmatrix} d\varepsilon_r^p \\ d\varepsilon_z^p \\ d\varepsilon_\theta^p \end{Bmatrix} = \begin{Bmatrix} 1 - \sin\psi \\ 0 \\ -1 - \sin\psi \end{Bmatrix}$$

Who is the law of flow with ξ a scalar to be determined?
We can then deduct the ratio plastic strains

$$\frac{d\varepsilon_r^p}{d\varepsilon_\theta^p} = -\frac{1-\sin\psi}{1+\sin\psi} = -n_\psi \tag{25}$$

We then deduct:

$$d\varepsilon_r^p = -n_\psi.d\varepsilon_\theta^p$$

$$\varepsilon_r^p = -n_\psi.\varepsilon_\theta^p + C_3$$

With C_3 constant independent of ϵ_θ and ϵ_r
From the mechanics of the continuous medium relations in axial symmetry, we have:

$$\frac{du}{dr} = -n_\psi.\frac{u}{r} + C_3 \tag{26}$$

Dilatancy decreases as the rock disaggregates. With the plastic radius r = c, the rock is intact with maximum dilatancy thus we will have:

$$\psi_{max} = \varphi - \varphi_\mu \tag{27}$$

With the plastic radius r = b, the rock is completely disaggregated and the dilatancy is null. We suppose a linear variation of dilatancy between the radius b and the radius c
This is shown in the (Table 1).
By putting $x = \frac{u}{r}$, the Eq 26 becomes:

$$x + \frac{dx}{dr}.x = -n_\psi + C_3$$

After integration, we obtain

$$-\frac{1}{1+n_\psi}\ln\left(\frac{\frac{u_b}{b}(1+n_\psi) - C_3}{\frac{u_a}{\alpha}(1+n_\psi) - C_3}\right) = \ln\frac{b}{a} \tag{28}$$

Table 1: Variation of friction and the dilatancy between the radius b and the radius c

Radius	Friction	Dilatancy	n_Ψ
c	φ	$\Psi = \varphi - \varphi_\mu$	$\frac{1-\sin\psi_{max}}{1+\sin\psi_{max}} = n_{\psi\,max}$
c	φ_μ	$\Psi = 0$	1

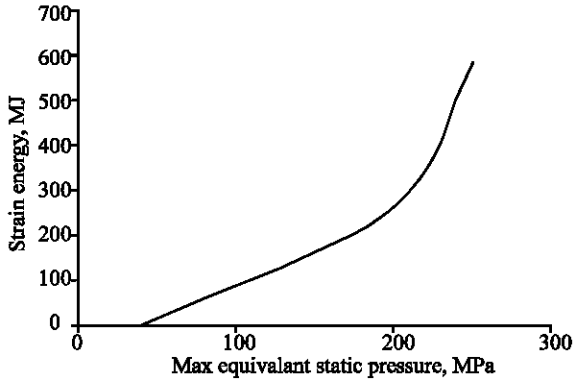

Fig .2: Variation of strain energy vs. max equivalent static pressure

Stress-strain relation: By combination of the relations 21 and 28 we obtain:

$$\frac{1}{1+n_\psi}\ln\left(\frac{\frac{u_a}{a}(1+n_\psi)-C_3}{\frac{u_b}{b}(1+n_\psi)-C_3}\right)=\frac{1}{N_f-1}.\ln\left(\frac{\sigma_{rb}}{p}\right) \quad (29)$$

From this Equation we can determine ' p', with $p = \sigma_{rb}$

$$\sigma_{rb}=p=\left[\frac{u_a}{a}(1+n_\psi-C_3)\right]^{\frac{1-N_f}{1+n_\psi}}.\frac{\sigma_{\theta b}}{\left[\varepsilon_{\theta b}(1-n_\psi)-C_3\right]^{\frac{1-N_f}{1+n_\psi}}} \quad (30)$$

The strain energy produced by ' p' to the radius level of drilling $r = \alpha$ is equal to

$$dw_\alpha=\sigma_{rb}.d\varepsilon_{r\alpha}+\sigma_{\theta\alpha}.d\varepsilon_{\theta\alpha}+\sigma_z.d\varepsilon_\alpha \quad (31)$$

Where $\sigma_z.d\varepsilon_\alpha=0$

From Eq 19 we can deduct:

$$dw_\alpha=\sigma_{rb}.d\varepsilon_{r\alpha}+N_f+\sigma_z.d\varepsilon_{\theta\alpha}$$

$$\varepsilon_r^p=-n_\psi\varepsilon_\theta^p+C_3$$

$$d\varepsilon_{r\alpha}^p=-n_\psi d\varepsilon_{\theta r}^p$$

$$dw_\alpha=\sigma_{rb}.d\varepsilon_{\theta\alpha}(N_f-n_\psi) \quad (32)$$

$$\varepsilon_{\theta\alpha}=\frac{u_\alpha}{\alpha}=\frac{1}{1+n_\psi}\left(\left(\frac{p}{\sigma_{rb}}\right)^{\frac{1+n_\psi}{1-N_f}}\left[\varepsilon_{\theta b}(1+n_\psi)-C_3\right]+C_3\right) \quad (33)$$

$$d\varepsilon_{\theta\alpha}=\frac{1}{1+n_\psi}\frac{p^{\frac{1+n_\psi}{1-N_f}}}{(\sigma_{rb})^{\frac{1+n_\psi}{1-N_f}}}\left[\varepsilon_{\theta b}(1+n_\psi)-C_3\right](N_f-n_\psi)dp \quad (34)$$

By introducing $\sigma_{ra}.d\varepsilon_{\theta a}$ into the formula 32 we obtain:

$$dw_{\theta\alpha}=p.\frac{1}{1+n_\psi}\frac{p^{\frac{1+n_\psi}{1-N_f}}}{(\sigma_{rb})^{\frac{1+n_\psi}{1-N_f}}}\left[\varepsilon_{\theta b}(1+n_\psi)-C_3\right](N_f-n_\psi)dp$$

$$w_\alpha=\frac{p^{\frac{n_\psi+2}{1-N_f}}}{n_\psi-N_f+2}.\frac{1}{(\sigma_{rc})^{\frac{1+n_\psi}{1-N_f}}}\left[\varepsilon_{\theta b}(1+n_\psi)-C_3\right](N_f-n_\psi) \quad (35)$$

Numerical application

$n_\Psi = 1$; $N_f=\frac{1-\sin\varphi_\mu}{1+\sin\varphi_\mu}$; $C=120*10^5$ Pa; $\rho=25000$ N; H=16.5m;

$E=19*10^{10}$Pa; $\nu=0.3$; $k_0=0.43$; $\varphi_\mu=36°$ Fig . 2 shows this numerical application

Calculation of dynamic energy related to the explosive mass: The energy of the explosion is the product of the quantity of explosive into the hole and that released per kilogram of explosive.

The quantity of explosive used on average by hole in Ouenza mine (Algeria) is about 150 kg with 10% of marmanite as priming and 90% of ANFO as principal charge with the principal characteristics which are represented below:

ANFO: density: 900 kg m^3; energy released by kg: 4 Mj

Marmanite: density: 960kg m^3; energy released by kg: 4.7 Mj

Total energy released: 610.5 MJ

From (Fig . 2) we can determine the equivalent pressure for a total released energy, we need a pressure of 205.75 for us MPa

From the formula (22) we determine the zone of great discontinuities radius which is equal to 6 m.

Calculation of the great discontinuities zone radius according to the blast parameters: The model of blasting requires the calculation of the great discontinuities zone radius, and the pressure on the inner sides of the hole.

The great discontinuities zone radius: The computation of the great discontinuities zone for coherent and friction rock takes into account the radius b which determines the limit between the destructuration zone and the zone of small cracks.

By integration of the equation (20) between r=a with the pressure ' p' applied to drilling and r = b, radial and tangential stresses in the destructuration zone will be

$$\sigma_{rb}=p\left(\frac{b}{a}\right)^{N-1} \quad (36)$$

$$\sigma_{\theta b}=N p\left(\frac{b}{a}\right)^{N-1} \quad (37)$$

In substituting the two expressions(36) and (37) in the Eq 8 will be:

$$b=a\left(\frac{2k_0\sigma_z}{p(N-1)}\right)^{\frac{1}{N-1}} \quad (38)$$

This expression can be written

$$b = a\left(\frac{p(N-1)}{2k_0\sigma_z}\right)^{\frac{1}{N-1}} \quad (39)$$

At the plastic radius b limit we still have an equilibrium, the radial and vertical stresses take respectively the values. P= p+C.ctg φ $\sigma_z=\sigma_z$+ C.ctgφ.

The expression 39 allows under these conditions to find the extension of great discontinuities the zone in a coherent and friction rock

$$b = r_t\left[\frac{(P+C.\,ctg\,\varphi)}{(1+\sin\varphi)(k_0\sigma_z+C.ctg\,\varphi)}\right]^{\frac{(1+\sin\varphi)}{2\sin\varphi}} (m) \quad (40)$$

Pressure on the inner sides of the hole

Detonation pressure: The detonation pressure (P_d) is given by[8]:

$$P_d = ¼\ ?_{ex}\ D^2 \quad (41)$$

ρ_{ex}: explosive density (Kg-m^3)
D: detonation velocity of the explosive (m/s)

Pressure on the inner sides of the hole: According to[9], the pressure on the inner sides of the hole is given by the following formula:

$$P = \frac{P_d\ volume.d'\ explosif}{2\quad volume.du.trou} \quad (42)$$

From the relations 41 and 42, we deduct:

$$P = \frac{1}{8}\rho_{ex}D^2\left(\frac{r_{ch}}{r^1}\right)^2\frac{l_{ch}}{l_t} \quad (43)$$

The explosive quantity into the hole (Q) is determined by the following formula

$$Q = q\ *l_{ch} \quad (44)$$

q: Linear charge of explosive kg/m

$$q = \pi\ r^2_t\rho_{ex}\left(\frac{r_{ch}}{r^1}\right)^2 \quad (45)$$

r_{ch} : explosive charge radius (m),

From the relations 43, 44 and 45 the pressure on inner sides of the hole can be deducted as follow:

$$P = \frac{1}{8}D^2\ \frac{Q}{l_t.\pi.r_t^2} \quad (46)$$

From the Eq. 40 and 46, the great discontinuities zone radius will be:

$$b = r_t\left[\frac{\left(\frac{D^2.Q}{8\pi l_t r_t^2}+C.ctg\,\varphi\right)}{(1+\sin\varphi)(k_0\sigma_z+C.ctg\varphi)}\right]^{\frac{(1+\sin\varphi)}{2\sin\varphi}} ;(m) \quad (47)$$

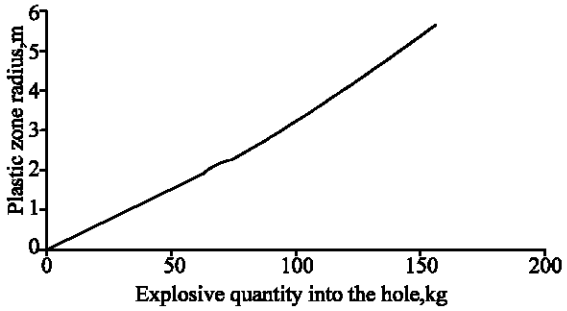

Fig. 3: Variation of plastic zone radius vs. explosive quantity into the hole

Numerical application :

Q = 150 kg hole; D= 3000 m s; C=120*10^5 Pa; φ =42°; r_t=0.075m; L_t =16.5m

According to the formula 47 the great discontinuities zone radius will be equal to 5.35m (Fig. .3)

EXPERIMENTATION ON SITE

A series of experimental works on drilling and blasting have been carried out an the Ouenza mine (Algeria). Its ground consists for overall of limestone alternating with fairly fractured marls.

The observations on the slope and upgrade bench do not allow specifying the importance of the fracturation due to the explosive. However the dimensions of solid mass disturbed zone constitute one of the principal indications on the influence of blasting on the bench stability. The exact limit determination of this zone has a great importance, especially during the realization of works close to the edges of the surface mines and the choice of the Optimal blasting pattern. The great and small discontinuities zones are formed at the back of the crater. The zone of great discontinuities is characterized by deep discontinuities on several meters varying from 0.02 to 0.7 m of opening. However, the small discontinuities zone are characterized by the presence of low discontinuities depth, the openings lower than 0.02m. Observations and measurements on the latter have been reposed on the basis of 17 blasts at the level of Ouenza mine Pic district (Fig .4 and Table 2).

The size of discontinuities decreases while moving away from the crater, with average opening size at several distances from the blasting as represented in Table 3.

Slope stability of bench in Ouenza mine: In practical application we are interested in a bench which volume in similar or slightly higher than the volume of broken rock by blast.

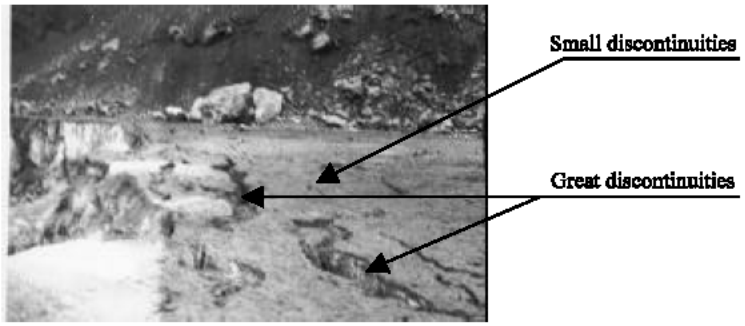

Fig. 4: Zone size after the blast

Table 2: Results of the 17 blast experiments

district Characteristics	Pic (17 tirs)
compressive strength (kgf cm^{-2})	600
Radius crater (m)	2 –3.5
Intermediate	2.57
variance	0.133
standard deviation	0.365
Great discontinuities radius (m)	4.2-7
Intermediate	5.5
variance	0.81
standard deviation	0.67

Table 3: Intermediate openings in the rock mass after the blast Distance from the blast

Opening (M)	(1 fracture/m) (cm)	Opening (2 fractures/m)(cm)
3,5	28	12
6	4	2
14	1	0.2

From the systematic observation of up grade bench, we can definite the potential failure surfaces which realistic appearance. They are made up of dominant failure, vertical, relatively developed sub parallel to the work face, after the blast. The geotechnical characteristics of this discontinuity are defined by shear testing using an LPC machine and specimen (60mm x 60mm), the applied normal stress are approximately situated between 2.5 and 5 bars and a low velocity of 0.5mm/h. The obtained results are as follow: null for cohesion and 35° for the friction angle.

Mechanical characteristics the intermediate plane : Between two planes, it is usual to consider a plane having the total characteristics of the solid rock mass (using at the same time the rock matrix and its discontinuity systems). But these values cannot be determined neither on sample nor in site.

They are then deducted from [10] ical laws which take into consideration: the dominant lithological nature of material and the solid rock mass state. The values for the cohesion and friction angle retained for Ouenza mine are respectively about 118 KPa and 36°, with a density of 25 KN^{-3}. Considering the very great difference between the laboratory test results and the computation by the semi empirical laws, the plane would have the same characteristics of a vertical discontinuity (C=0 and φ_F5°) for the considered extreme case. The most critical static situations on profiles including a bench are represented in Table 4

The influence of studied vertical crack position is respectively:

- rom 2m or 4m at the top of the slope.
- 2m and more than half of the bench height for an inclination angle of fissure θ varying from 40° to 80°

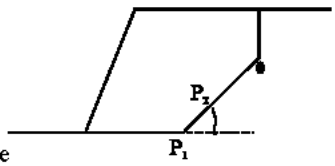

P_1: bedding plane
P_2: intermediate plane

In the first case the safety coefficient (Fstatic) is weak and lower than 1.02 whatever the depth and the position of the vertical fissure, for the second case the safety coefficient is higher than 2.7.

Table 4 : Values of θ and F_{static} for the critical cases.

		Discontinuities at 2 m of edge				Discontinuities at 2 m of edge			
Number of bench	Depth of discontinuities	Case 1		Case 2		Case 1		Case 2	
1	2	60	1.00	80	5.59	45	0.85	71	3.47
	4	55	0.78	76	4.8	48	0.98	68	3
	6	52	0.79	72	3.79	50	1.01	60	2.8
	8	47	0.83	65	3.08	55	0.92	42	2.7

CONCLUSIONS

The main conclusions which can be drawn areas follow:

- Determination of the static pressure generated by the dynamic energy of the blast and the static energy of equivalent strain starting from a model of calculation based on an elastoplastic behaviour
- Determination of the great discontinuity zones radius according to the equivalent static pressure and the blast parameters.
- Determination of the great discontinuity zones radius on the basis of the explosive energy, and in site blast parameters.
- The safety coefficient is low for a vertical discontinuity (C=0 and φf=35°), and increases with the depth of the back fissure.
- At the opposite of the characteristics of the solid mass resulting from Hoek and Brown empirical laws, the safety coefficient is raised and becomes more significant when the fissure is reduced.

ACKNOWLEDGEMENTS

The authors are indebted to Mr Jacques Monnet laboratory for LIRIGM Grenoble and the staff of Ouenza mine for theirs suggestions.

REFERENCES

1. Sadwin, L.D. and N.M. Junk, 1965. Measurements of lateral pressure generated from Cylindrical Explosive charges. U.S Bureau Min. R.I., pp: 6701- 8.
2. Ortiz, R. and M. Tijani, 2002. Quantification de l'énergie transférée à la roche lors du tir à l'explosif : Elaboration d'une technologie. Les Techniques de l'Industrie Minérale, 13: 127-132
3. Atchison, T.C., 1968. In: Pfleicher E.P. (Ed.). Fragmentation Principles In Surface Mining. AIME. pp: 355- 372
4. Monnet, J. and T. Chema, 1994. Etude théorique et expérimentale de l'équilibre élasto-plastique d'un sol cohérent autour d'un pressiomètre. Revue Française de Géotechnique,73: 15-27
5. Dowding, C.H., G.A. Nicholson, P.A. Taylor, A. Agoston and C.E. Pierce, 1996. Recent Advancements in TDR Monitoring of Ground Water Levels and Piezometric Pressures. Rock Mechanics Tools and Techniques: Proceedings of the 2nd North American Rock Mechanics Symposium. Montreal, Quebec
6. Obert, L. and W.L. Duvall, 1967. Rock Mechanics and the design of structures in Rock, Pub. J. Wiley and Sons, Inc.
7. Monnet, J. and J. Khlif, 1994. Etude théorique et expérimentale de l'équilibre élasto-plastique d'un sol pulvérulent autour d'un pressiomètre. Revue Française de Géotechnique, 66: 71-80
8. Thiard, R. and A. Blanchier 1984. Evolution des systèmes d'amorçages. Revue de l'Industrie Minérale, les Techniques, Mines et Carrières pp: 113-119.
9. Yamauchi, H., T. Matsumodo and S. Kamega, 1980. An example of presplitting using slurry. Explosive. J. the Industrial Explosives Society, Japan, 41: 306-310.
10. Hoek, E. and J.W. Bray, 1977. Rock slope engineering. The Institution of Mining and Metallurgy London, pp: 283-284.